

Construction and characterization of a truncated tissue factor-coagulation-based composite system for selective thrombosis in tumor blood vessels

PEILAN XU, MINGYUAN ZOU, SHENGYU WANG, TINGTING LI, CONG LIU,
LI WANG, LANLAN WANG, FANGHONG LUO, TING WU and JIANGHUA YAN

Cancer Research Center, School of Medicine, Xiamen University, Xiamen, Fujian 361102, P.R. China

Received March 27, 2019; Accepted July 24, 2019

DOI: 10.3892/ijo.2019.4855

Abstract. The selective induction of tumor vascular thrombosis using truncated tissue factor (tTF) delivered via a target ligand is a promising novel antitumor strategy. In the present study, an anti-neuropilin-1 (NRP-1) monoclonal antibody (mAb)-streptavidin (SA):tTF-biotin (B) composite system was established. In this system, anti-NRP-1-mAb located tTF to the tumor vascular endothelial cell surface and induced vascular embolization. Due to their high binding affinity, SA and B were used to enhance thrombogenic activity. mAb was conjugated with SA using a coupling method with water-soluble 1-ethyl-3-(3-dimethylaminopropyl) carbodiimide and N-hydroxysulfosuccinimide. Biotinylated tTF (tTF-B) was prepared using a B-labeling kit subsequent to the generation and purification of fusion protein tTF. Confocal microscopy and flow cytometry indicated that the anti-NRP-1-mAb-SA conjugate retained mAb targeting activity. The preservation of B-conjugate binding capacity was confirmed using a competitive ELISA, and factor X-activation analysis revealed that tTF-B retained the procoagulant activity exhibited by tTF. Live imaging was performed to assess mAb-SA distribution and tumor-targeting capability, and this yielded promising results. The results of *in vivo* studies in mice with subcutaneous xenografts demonstrated that this composite system significantly induced tumor vascular thrombosis and inhibited tumor growth, whereas these histological changes were not observed in normal organs.

Introduction

Tumor progression and metastasis relies on the delivery of sufficient oxygen and nutrients via blood vessels (1). Selectively inducing thrombosis in tumor vasculature, leading to tumor infarction, is an effective and promising antitumor strategy (2). Over the past 20 years, encouraging research into a new vascular targeting therapy has emerged (3,4). In this strategy, truncated tissue factor (tTF) is used as a mediator and an extracellular domain of tissue factor (TF). TF is a major initiator of thrombogenic cascades (5). As a recombinant form of TF, tTF only contains the cell surface domain and exhibits less (1×10^5) factor X activity compared with TF in the phospholipid membrane (6). Both the intrinsic and extrinsic blood coagulation pathways lead to activation of coagulation factor X (7); activated factor X then converts prothrombin to thrombin, which finally accumulates in the generation of fibrin polymers and blood clots. tTF exhibits limited ability to activate factor X; however, tTF can recover its native function and initiate local thrombosis once bound to the cell surface (negatively charged phospholipid) using a targeting agent (8). This targeting agent may be an antibody or a peptide ligand. Numerous biochemical conjugates and recombinant fusion proteins associated with tTF have been synthesized, and have been demonstrated to exhibit potential antitumor activity (9,10). However, the use of tTF-ligand has certain limitations. Due to the low affinity of the targeting moiety in tumors, the undesirable tumor-specific targets often fail to induce complete thrombosis (11). Identification of additional targeting ligands or tumor-specific receptors may be required to enhance therapeutic efficacy.

Neuropilin-1 (NRP-1) is a non-tyrosine kinase transmembrane receptor of 120-130 kDa. This glycoprotein, first characterized as the receptor of neuronal semaphorin 3A, was subsequently revealed to be a co-receptor of vascular endothelial growth factor (VEGF)₁₆₅ (12). Therefore, NRP-1 may indirectly enhance the biological activities of VEGF, including promoting the migration and angiogenesis of human umbilical vein endothelial cells (HUVECs) (13). Furthermore, NRP-1 expression has been revealed to be upregulated in a variety of tumor types, including hepatocellular carcinoma and breast cancer, and has been associated with poor

Correspondence to: Dr Jianghua Yan or Dr Ting Wu, Cancer Research Center, School of Medicine, Xiamen University, 422 Xiangan South Road, Xiamen, Fujian 361102, P.R. China
E-mail: jhyan@xmu.edu.cn
E-mail: wuting78@aliyun.com

Key words: vascular targeting therapy, anti-neuropilin-1 monoclonal antibody, truncated tissue factor, streptavidin-biotin system, thrombosis

prognosis (14-16). Due to the association of NRP-1 with tumor promotion, NRP-1 appears to be a promising angiogenesis target. However, conjugated antibody-tTF often cannot induce complete thrombosis due to this antibody only solving the issue of specific delivery (17,18). The distribution of vascular targets (antigens or receptors) in the tumor vasculature is a major factor affecting tTF concentration (19). In the present study, the accumulation of tTF in tumor blood vessels was increased using the streptavidin (SA)-biotin (B) system, which was introduced to promote coagulation efficiency.

SA is a 60-kDa tetrameric protein generated from *Streptomyces avidinii*, and is commercially available at a high purity and exhibits favorable *in vivo* stability (20,21). The binding affinity of SA for B, a 244-kDa vitamin, is high ($K_d=10^{-15}$ mol/l) (22). Due to the rapid association and strong interaction between SA and B, these molecules have been widely used as binding pairs in analysis, drug delivery systems and pre-targeting radioimmunotherapy (23-28).

In the present study, a novel tumor vasculature-targeting approach was explored. This strategy consisted of an SA-conjugated anti-NRP-1 monoclonal antibody (mAb-SA) and biotinylated tTF (tTF-B). Anti-NRP-1 mAb (mAb), which was previously generated via the hybridoma technique in the laboratory (29), was conjugated to SA to pre-target the NRP-1 receptors on the tumor vascular endothelial cell surface. mAb-SA diffused into the tumor area, and tTF-B was subsequently administered and efficiently combined with mAb-SA to induce local tumor thrombosis. To explore the therapeutic feasibility of this two-step coagulation approach, *in vitro* studies were performed to assess the targeting ability of mAb-SA and procoagulant activity of tTF-B, and to compare the B/SA binding capacity between mAb-SA and tTF-B. Live imaging was used to investigate the distribution and *in vivo* tumor-binding ability of mAb-SA. Antitumor activity and coagulation efficiency was subsequently evaluated via *in vivo* assessments and histological analysis.

Materials and methods

Materials. Anti-NRP-1 mAb with a high purity was produced using the hybridoma technique and preserved in the laboratory after freeze-drying (29). 2-(N-morpholino) ethane sulfonic acid (MES), 1-ethyl-3-(3-dimethylaminopropyl) carbodiimide (EDC), N-hydroxysulfosuccinimide (sulfo-NHS), streptavidin (SA), Sephadex G200 and a Sephadex G200 column (1.5x22 cm) were purchased from Sigma-Aldrich (Merck KGaA). GoldBand 3-color Regular Range Protein Marker (10-180 kDa) was purchased from Shanghai Yeasen Biotechnology Co., Ltd. Endothelial cell medium (ECM) containing human epidermal growth factor was purchased from Shanghai Zhong Qiao Xin Zhou Biotechnology Co., Ltd. DMEM and FBS were purchased from Invitrogen (Thermo Fisher Scientific, Inc.). Mouse IgG isotype (cat. no. 0107-01) was obtained from AmyJet Scientific Inc. Rhodamine B isothiocyanate (RBITC)-conjugated goat anti-mouse IgG (cat. no. D111097), isopropyl-1-thio-B-d-galactopyranoside (IPTG), BSA, Hoechst 33258 powder, and hematoxylin and eosin (H&E) were purchased from Sangon Biotech Co., Ltd. Factors X and VII were obtained from Sigma-Aldrich (Merck KGaA). pET22b (+) plasmid and *E. coli* BL21(DE3) were

purchased from Novagen (Merck KGaA). cDNA encoding for tTF, containing amino acids 1 to 218 of human TF, was used to generate the tTF expression vector tTF-pET22b (+) via PCR using the following primers: Forward, 5'-TCCATGGGC TCTGGCACTACA-3' and reverse, 5'-GTGCTCGAGTTC TCTGAATTCC-3'. *Nco*I and *Xho*I restriction enzymes were used to insert cDNA into the plasmid. Nickel-nitrilotriacetic acid (Ni-NTA) agarose was purchased from Qiagen, Inc. A B-labeling kit was obtained from Wuhan Elabscience Biotechnology Co., Ltd. Cyanine-5 (Cy5) NHS-ester was purchased from Tiangen Biotech Co., Ltd.

Preparation of mAb-SA conjugate. The purity of anti-NRP-1 mAb was first identified via 12% SDS-PAGE. As presented in Fig. 1, the mAb-SA conjugate was synthesized using a coupling method (30). The concentration of mAb was adjusted to 3 mg/ml with reaction buffer (0.1 mol/l MES; 0.5 mol/l NaCl; pH 6.0) according to the improved Bradford method. A total of 3.83 mg (0.02 mmol) of EDC and 4.34 mg (0.02 mmol) of sulfo-NHS were weighed and immediately transferred to the reaction solution (1 ml). The solution was mixed and stirred at room temperature for 15 min. SA concentration was adjusted to 1.2 mg/ml with 0.1 mol/l potassium phosphate buffer (pH 7.5), and 1 ml SA was added to the reaction buffer. Nitrogen gas was purged into the solution for 3 min and the beaker was then sealed. The reaction was subsequently left to proceed at room temperature for 2 h, then purified using a Sephadex G200 column as previously described (31,32), with some modifications. Briefly, Sephadex G200 was swelled in a boiling water bath for 2 h and cooled. Pretreated Sephadex G200 was poured into the column slowly, with no air mixing in, and equilibrated with pure water (pH 7.5) for 40 min. The crude product was then slowly added to the column and eluted with pure water at a rate of 0.2 ml/min. Eluted samples (1.5 ml/tube) were collected and read with a NanoDrop™ 2000 spectrophotometer (NanoDrop Technologies; Thermo Fisher Scientific, Inc.) at 280 nm. All purification steps were conducted at 4°C. Native 8% PAGE was performed to confirm whether conjugated protein had been successfully isolated (33).

Cell culture. HUVECs and the human liver cancer cell line HepG2, which both overexpress NRP-1 (34,35), were obtained from the American Type Culture Collection. HUVECs were used for *in vitro* experiments, and HepG2 cells were used to establish a mouse tumor model. HepG2 cells were cultured in high-glucose DMEM supplemented with 1% penicillin-streptomycin and 10% FBS. HUVECs were cultured in ECM containing human epidermal growth factor. All cells were incubated in a humidified atmosphere with 5% CO₂ at 37°C.

Confocal immunofluorescence. HUVECs (1x10⁵ cells/ml) were seeded into a 6-well culture plate with one glass coverslip per well. The cells were then incubated and subsequently washed with PBS (pH 7.4) three times, until 50% cloning efficiency had been reached. The cells were then fixed with 1 ml 4% paraformaldehyde at 4°C for 30 min and washed with PBS three times. A total of 2 ml PBS containing mAb, mAb-SA or a mouse IgG isotype control (1:5,000) was added, and the cells were cultured at 37°C for 1 h. After washing, cells were cultured with a goat anti-mouse RBITC mAb (1:200) at 37°C

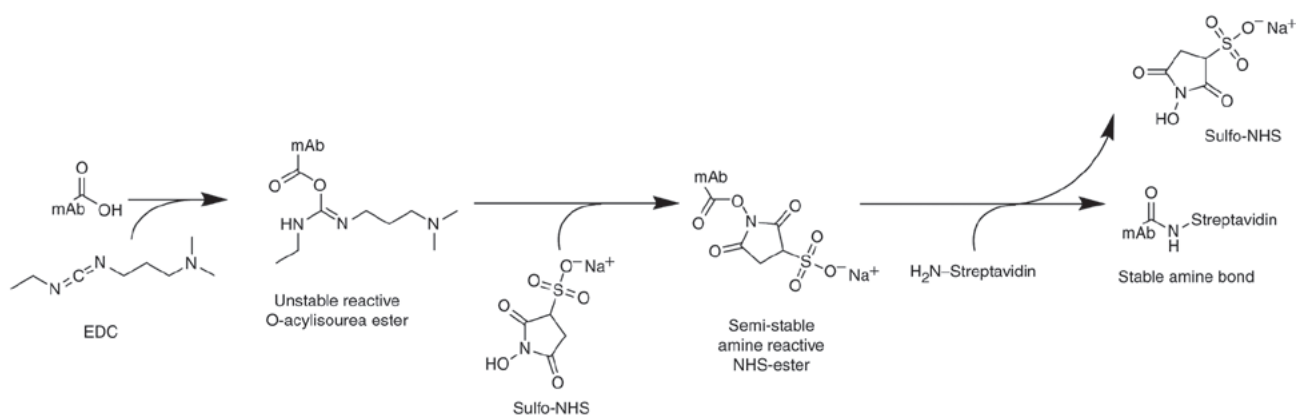


Figure 1. Formation of the mAb-SA conjugate via the EDC reaction. SA was conjugated to mAb using a two-step cross-linking procedure with zero-length heterobifunctional cross-linkers. mAb, monoclonal antibody; SA, streptavidin; EDC, 1-ethyl-3-(3-dimethylaminopropyl) carbodiimide; sulfo-NHS, N-hydroxysulfosuccinimide.

for an additional 1 h in the dark. Hoechst 33258 was used to stain cell nuclei at 37°C for 5 min and the samples were then examined under a FV1000MPE-B confocal microscope (Olympus Corporation) and photographed. Five random fields per sample were analyzed (magnification, x600).

Flow cytometry. Semiquantitative analysis was conducted to further assess the ability of the mAb-SA conjugate to target NRP-1. HUVECs were removed from the culture plate using trypsin and washed with PBS three times. The cells were then fixed with 1 ml 4% paraformaldehyde at 4°C for 30 min and washed with PBS three times. After being resuspended in PBS, cells were incubated with mAb, mAb-SA or the mouse IgG isotype (1:5,000) control at 37°C for 1 h and incubated with the anti-mouse RBITC mAb (1:200) at 37°C for a further 1 h. Each sample of 10,000 cells was analyzed using a CytoFlex S flow cytometer (Beckman Coulter, Inc.). Results were analyzed using CytExpert version 2.0 (Beckman Coulter, Inc.).

Production of fusion protein tTF. *E. coli* (BL21; DE3) containing tTF expression vector were cultured in Luria broth supplemented with 1% ampicillin. IPTG was added when the germiculture reached 0.6-0.8 at 600 nm to induce the expression of the fusion protein tTF. After stimulation for 6 h, bacterial cells were collected and centrifuged at 12,000 x g at 4°C for 20 min. A total of 5 ml lysis buffer (20 mmol/l Tris/HCl; pH 8.0; 0.5 mol/l NaCl; 2 mol/l urea; 20 ml/l Triton X-100) per gram (wet weight) was subsequently added. After incubating for 90 min, cells were centrifuged at 12,000 x g for 20 min at 4°C. The pellet was resuspended and sonicated (sonication time: 5 sec; interval time: 5 sec) in washing buffer (20 mmol/l Tris/HCl; pH 8.0; 0.5 mol/l NaCl; 2 mol/l urea; 20 ml/l Triton X-100) at 4°C for 30 min. A total of 5 ml solubilization buffer (20 mmol/l Tris/HCl; pH 8.0; 8 mol/l urea; 1 mmol/l β-mercaptoethanol; 20 ml/l Triton X-100) per gram (wet weight) was added to dissolve the inclusion bodies. After incubation at room temperature overnight, the suspension was centrifuged at 12,000 x g for 20 min at 4°C. The supernatant was then purified with a Ni-NTA column according to the protocol of the His-Bind Buffer kit (Novagen; Merck KGaA). The products were analyzed using 12% SDS-PAGE under

denaturing conditions. The purified fusion protein tTF was then concentrated using a Centrifugal Filter and freeze-dried for subsequent use.

Factor X activation. tTF-B was prepared using a B-labeling kit according to the manufacturer's protocol. A factor X activation assay was performed to assess the coagulation activity of tTF-B, as previously described (36). Various concentrations (0.01-10 μmol/l) of BSA, tTF or tTF-B were incubated with 100 nmol/l factor VII in Tris-buffered saline at 37°C for 10 min. Factor X (5 nmol/l) was then added, and the mixture was incubated for 10 min at room temperature. The reaction was subsequently quenched using 100 mmol/l EDTA. A total of 2 nmol/l Spectrozyme FXa was added to the mixture, and the absorbance was detected at 405 nm after 3 min.

ELISA. A competitive ELISA was performed to determine the B/SA-binding capacity of mAb-SA/tTF-B. A 96-well plate was coated with tTF-B (100 μl/well; 20 μg/ml) in coating buffer (7.5 mM sodium carbonate; 17.4 mM sodium bicarbonate; pH 9.6) and incubated overnight at 4°C. The plate was then washed three times with PBS-Tween solution (0.01 mol/l, pH 7.4, 0.05% Tween-20), and 10% FBS was then used to block the unbound sites at 37°C for 1 h. After washing the plate five times, HRP-labeled SA (100 μl/well; 200 μg/ml) and was added to each well to serve as the competitor. Serially diluted mAb-SA or SA (100 μl/well; 200-12.5 μg/ml) was then added separately. After incubation for 1 h at 37°C, the enzyme substrate orthophenylenediamine, in 50 mM phosphate-citrate buffer (pH 5.0 with fresh 30% hydrogen peroxide) and at a concentration of 0.4 mg/ml, was added (100 μl/well). The plate was subsequently incubated at room temperature for 20 min, and 1 M H₂SO₄ was added to quench the reaction (50 μl/well). Absorbance values were measured at 490 nm. The inhibition rate was calculated according to a previous study (37) to determine the immunoreactivity of mAb-SA.

Mouse tumor models. Female BALB/c nude mice (n=60, 6-8 weeks old, 18-22 g) were purchased from the Experimental Animal Center of Xiamen University, of which 52 were

ultimately used for experiments. HepG2 cells were dissociated in a culture plate using 10% trypsin at 37°C for 3 min, and subsequently resuspended in PBS. Each mouse was then subcutaneously injected in the right flank with 100 μ l HepG2 cells (1×10^6). Animals were housed in the Experimental Animal Center under specific pathogen-free conditions: Temperature, 22–25°C; humidity, 50–60%; 12-h light/dark cycle. Mice had free access to water and Purina 5L79 rodent chow. Animal health and behavior were monitored daily. Animal welfare was in accordance with institutional guidelines. When the mean tumor volume [calculated as $(\text{length} \times \text{width}^2)/2$] reached 150–250 mm³, those mice were used for live imaging, antitumor activity studies and histological analysis after being acclimatized. The largest subcutaneous tumor observed in the present study was 1.9 cm in diameter at its widest point, and no mice exhibited multiple subcutaneous tumors. According to a previous study (38), the humane endpoints were determined based on the mouse weight loss (>20% of total body weight) or mouse activity assessment (hunching, stationary, ruffling and poor grooming), and mice were euthanized via cervical dislocation and dissected. The duration of the animal experiment was ~25 days. Then, all remaining mice were euthanized by cervical dislocation, and no mice were found dead. All animal experiments performed in the present study were approved by the Ethics Committee of Xiamen University.

Fluorescent labeling. SA, anti-NRP-1 mAb and mAb-SA were labeled with fluorescein. The concentration of Cy5 NHS-ester used was 1 mg/ml in DMSO. According to the total amount of proteins (SA, anti-NRP-1 mAb or mAb-SA), 0.01 mg fluorescein per mg protein were mixed at room temperature for 2 h. Dialysis was performed to remove unlabeled Cy5 NHS-ester for 4 h at room temperature and subsequently at 4°C overnight with 0.15 mol/l NaCl solution. The whole process was performed in the dark.

In vivo imaging. To investigate the *in vivo* distribution of mAb-SA, nude mice with subcutaneous xenografts were randomly divided into four groups ($n=3/\text{group}$). Mice in each group were intravenously injected with 100 μ l saline, SA-Cy5, anti-NRP-1 mAb-Cy5, or mAb-SA-Cy5 via the tail vein. After the mice were anesthetized in 1.5% isoflurane, the Cy5 fluorochrome was then detected in mice using an Imaging IVIS-200 system (PerkinElmer, Inc.) at 0.5, 3, 6, 12, 24, 36, 48 and 72 h. The nude mice were sacrificed after imaging. Tumor tissues and major organs, including the heart, liver, spleen, lungs, kidneys and brain, were isolated from the mAb-SA-Cy5 treatment group, and their fluorescent signal intensity was measured using Living Image version 4.3 (Caliper Life Sciences, Inc.; PerkinElmer, Inc.).

Antitumor efficacy evaluation. Nude mice bearing 150 ± 50 mm³ HepG2 tumors were randomly assigned to four groups ($n=10/\text{group}$). Mice in each group received four intravenous administrations of saline, mAb-SA, tTF-B and mAb-SA:tTF-B, at 3-day intervals, at a dose of 5 mg/kg. In the mAb-SA:tTF-B treatment group, tTF-B was injected 24 h after each administration of mAb-SA. Tumor size was measured every second day. Tumor tissues were surgically removed and weighed after 12 days of treatment.

Histological analysis. To evaluate the tumor vascular targeting ability of the mAb-SA:tTF-B composite system and its effects on intravascular thrombosis *in vivo*, tumors from different treatment groups and major organs from the mAb-SA:tTF-B group were fixed in 4% formaldehyde solution at room temperature for 48 h before embedding in paraffin and cutting into 5–7- μ m sections for Harris H&E staining. Tissues were stained with hematoxylin and eosin at room temperature for 3 min and 20 min, respectively. Five random fields per sample were examined under a light microscope (magnification, $\times 200$).

Statistical analysis. All data in the present study were analyzed using Prism 6.0 (GraphPad Software, Inc.) and presented as the mean \pm standard deviation. One-way ANOVA with Tukey's multiple comparison post hoc test was performed to assess the differences among groups. $P < 0.05$ was considered to indicate statistically significant differences.

Results

Preparation of mAb-SA conjugate via EDC reaction and purification using gel-filtration. As presented in Fig. 2A, the purity of anti-NRP-1 mAb reached ~95%. To separate the desired synthetic product from any impurities, including the cross-linked byproduct, any unreacted antibodies and the unreacted SA, the crude products were purified using a Sephadex G200 gel-filtration column, which was washed using pure water (pH 7.5). To avoid dissociation to monomeric species, the conjugate was analyzed using native 8% PAGE under a non-boiled condition. The bands shown in Fig. 2B correspond to (from left to right) unreacted SA, unreacted mAb and conjugate products after purification. The final purified conjugate was well-defined and clear.

Confocal immunofluorescence and flow cytometry demonstrate the in vitro NRP-1 targeting ability of mAb-SA. Confocal immunofluorescence and flow cytometry were performed to determine whether mAb-SA maintained biological targeting activity. As presented in Fig. 3A, red fluorescence of RBITC was observed on the surface membrane of HUVECs treated with mAb or mAb-SA. This result indicated that mAb-SA was able to bind with NRP-1 on the cell surface. The results of flow cytometry (Fig. 3B) were similar to those of the confocal experiment. The anti-NRP-1 mAb and mAb-SA groups exhibited significant HUVEC-binding activity. The NRP-1-binding capacity of mAb-SA was almost equivalent to that of mAb.

Preparation and purification of tTF fusion protein. To optimize the culture conditions, various concentrations (0–1 mmol/l) of IPTG were used. 12% SDS-PAGE was performed to evaluate the induced fusion protein yield (Fig. 4). A maximum yield was observed when the IPTG concentration reached 0.8 mmol/l. The fusion protein was expressed in the form of inclusion bodies. The inclusion bodies were washed with washing buffer and subsequently dissolved in denaturation buffer. A nickel affinity column was used to purify the soluble products. As presented in Fig. 4, the objective fusion protein was ~34 kDa with ~99% purity.

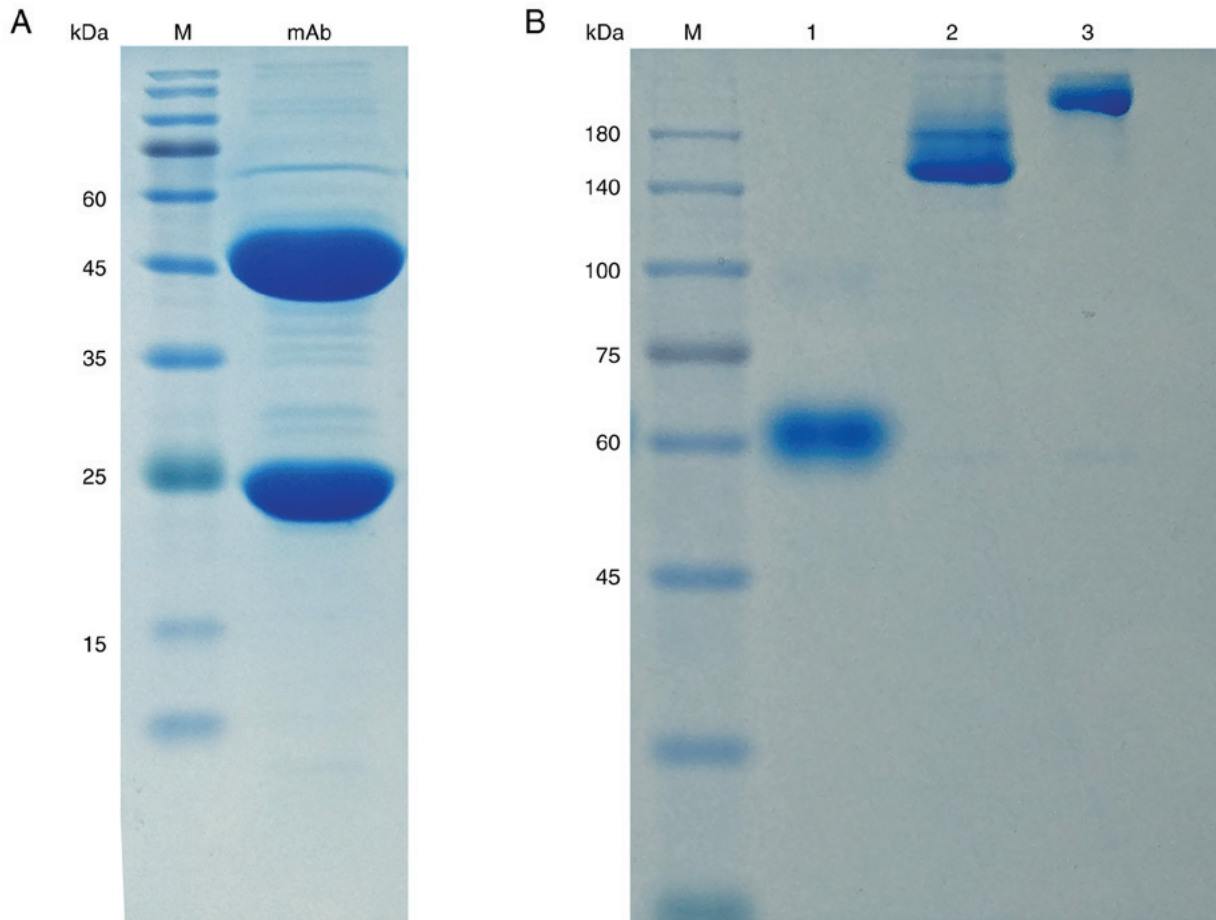


Figure 2. Preparation and purification of mAb-SA. (A) SDS-PAGE analysis showed that the purity of anti-NRP-1 mAb reached ~95%. Heavy and light chain bands were observed at ~45 and ~25 kDa, respectively. (B) Synthetic products were characterized using native 8% PAGE. Lane 1, SA (60 kDa) before conjugation; lane 2, anti-NRP-1 mAb (~150 kDa) before conjugation; lane 3, final purified conjugate mAb-SA (~210 kDa). mAb, monoclonal antibody; SA, streptavidin; NRP-1, neuropilin-1; M, protein marker.

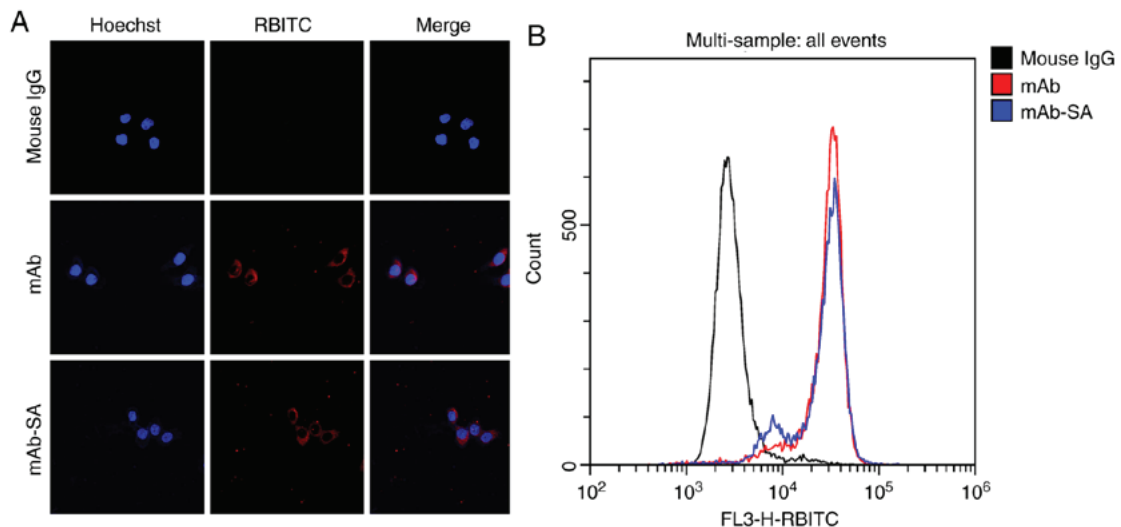


Figure 3. Functional characterization of mAb-SA. (A) Targeting ability of mAb-SA was analyzed using confocal immunofluorescence. mAb and mAb-SA bound to the surface of HUVECs, whereas the negative control (mouse IgG) did not. (B) Flow cytometry was performed to further evaluate the targeting capacity of mAb-SA. Cell count curves with different fluorescence intensities were shown. mAb (red curve); mAb-SA (blue curve); negative control (black curve). RBITC, Rhodamine B isothiocyanate; mAb, monoclonal antibody; SA, streptavidin; HUVECs, human umbilical vein endothelial cells.

tTF-B promotes blood coagulation in vitro. A factor X activation assay was performed to evaluate the retention of blood

coagulation activity in tTF-B. As presented in Fig. 5, tTF and tTF-B exhibited similar factor X activity at the corresponding

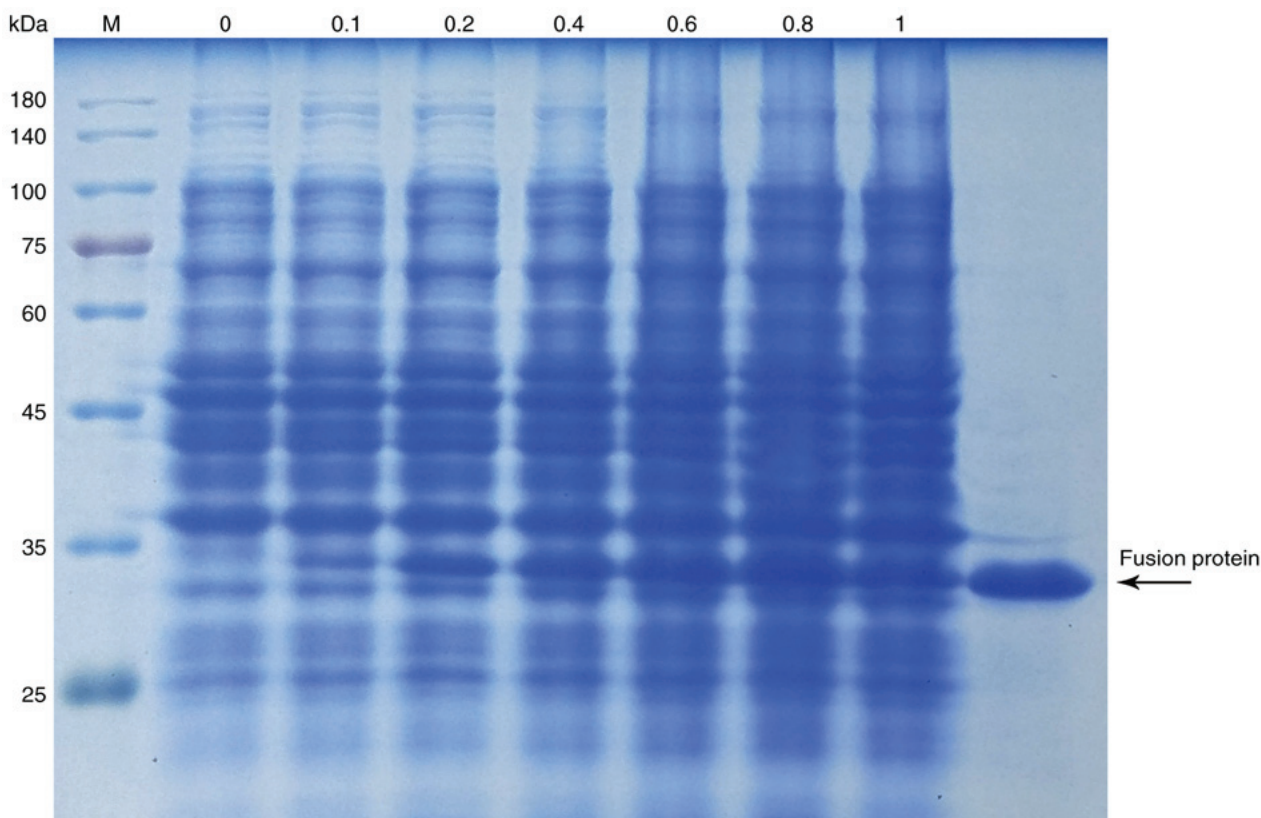


Figure 4. SDS-PAGE analysis of the expression and purification of the fusion protein tTF. Lane 2-8, total proteins induced by IPTG at a concentration of 0, 0.1, 0.2, 0.4, 0.6, 0.8 and 1 mmol/l, respectively; lane 9, final fusion protein tTF purified with a nickel affinity column. tTF, truncated tissue factor; M, protein marker.

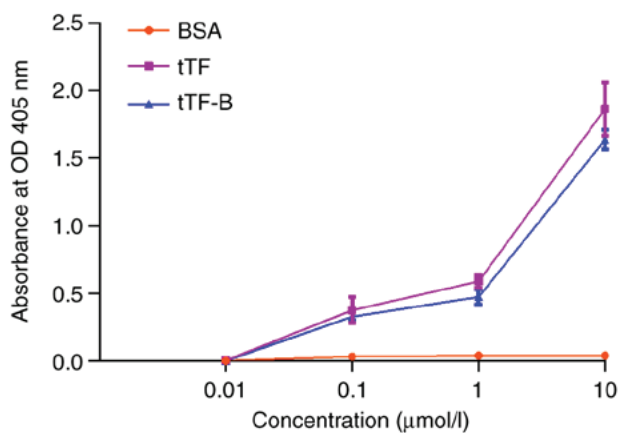


Figure 5. Factor X coagulation assay. The ability of tTF-B and control protein tTF to facilitate the specific proteolytic activation of factor X by factor VII was assessed using a factor X coagulation assay; BSA was used as the negative control. The tTF-B retained the ability of the tTF moiety to induce blood coagulation. tTF, truncated tissue factor; B, biotin; OD, optical density.

concentrations, indicating that tTF-B retained the tTF moiety when inducing blood coagulation.

Verification of B/SA binding ability. A competitive ELISA was used to detect the *in vitro* binding ability of tTF-B and mAb-SA (Fig. 6). The results revealed that the EDC reaction did not impair the B-binding ability of SA. The tTF-B-binding capacity of the mAb-SA conjugate was 73% compared with

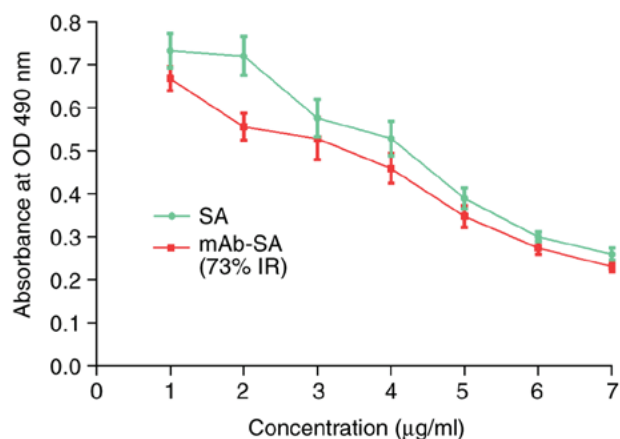


Figure 6. Competitive ELISA of SA vs. mAb-SA on tTF-B. Competitive ELISA was performed to determine the tTF-B-binding capacity of SA/mAb-SA. The tTF-B-binding capacity of mAb-SA conjugate was 73% relative to that of unmodified SA. mAb, monoclonal antibody; SA, streptavidin; tTF, truncated tissue factor; B, biotin; OD, optical density; IR, inhibition rate.

that of unmodified SA. Therefore, the *in vitro* use of the mAb-SA:tTF-B system may also be of value for *in vivo* studies.

***In vivo* distribution of mAb-SA.** Live imaging was performed to assess the distribution of mAb-SA in tumor-bearing mice. A variety of Cy5-labeled reagents and saline (blank control) were intravenously injected, and the fluorescent signals were

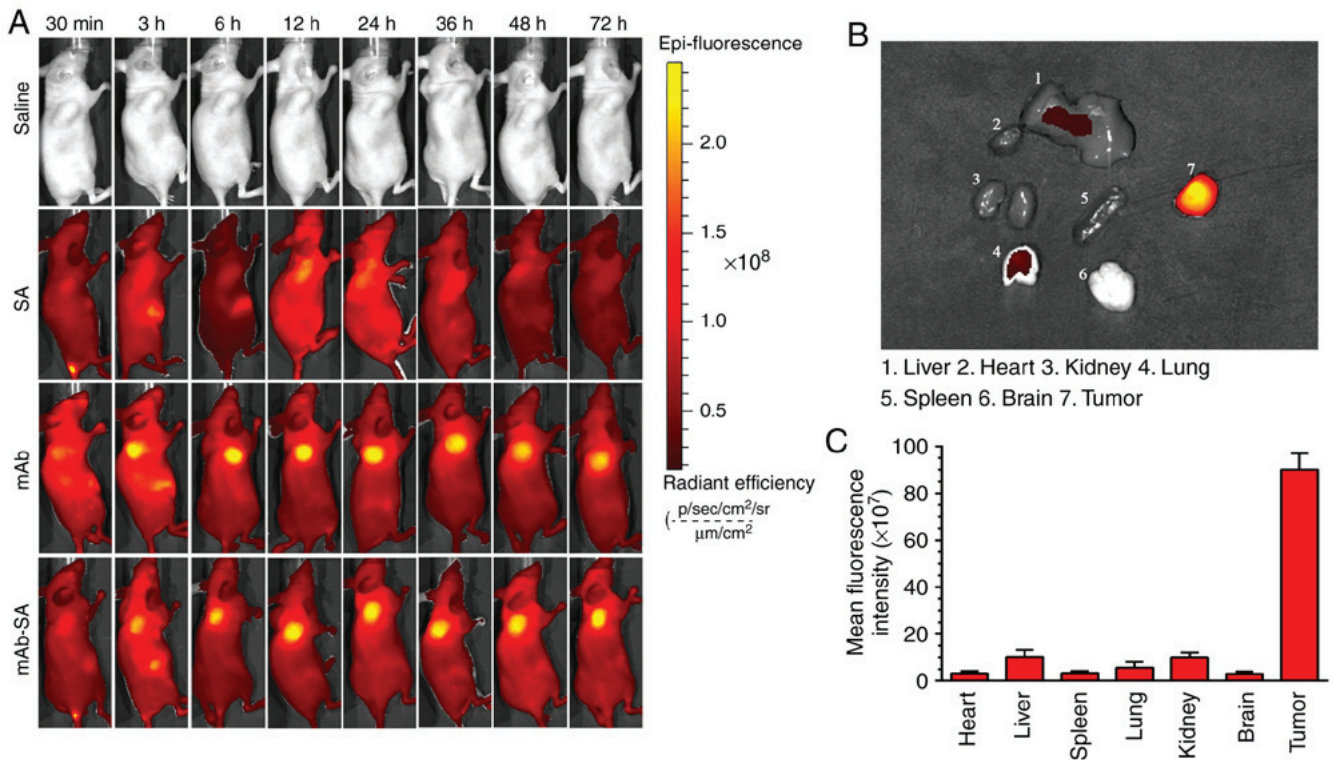


Figure 7. Representative live imaging of Cy5-labeled agents in tumor-bearing mice. (A) *In vivo* imaging of HepG2 xenograft-bearing nude mice at various time points following administration of saline, SA, mAb and mAb-SA. (B) Fluorescence imaging of major normal organs and tumor tissues from the mAb-SA-Cy5 treatment group at 72 h following administration. (C) Mean fluorescence intensities of major organs and tumors from the mAb-SA-Cy5 treatment group. mAb, monoclonal antibody; SA, streptavidin; Cy5, cyanine-5.

detected at various time points. As presented in Fig. 7A, Cy5-labeled mAb and mAb-SA were detected in the tumor area at 3 h following intravenous injection. The peaks in fluorescent signals were similar at 24 h; however, no SA-Cy5 fluorescent signal was observed in tumor tissues. The fluorescent signals in the mAb and mAb-SA-Cy5 treatment groups remained strong at 72 h (Fig. 7B and C). Weak Cy5 fluorescence signals were detected in the major organs; the fluorescence intensity ratio of tumor to non-tumor tissue was ~ 8.83 - 29.80 in mice injected with mAb-SA-Cy5. The results of the present study suggested that the mAb-SA conjugate was able to selectively target tumor tissues, but was not retained by normal organs.

Antitumor activity of the mAb-SA:tTF-B system. The antitumor activity of the mAb-SA:tTF-B system was evaluated in HepG2 xenograft-bearing nude mice. Tumor growth curves are presented in Fig. 8A. Overall, tumors in mice treated with mAb-SA:tTF-B exhibited decreased growth compared with other treatment groups. Tumor regression was also only observed following the third treatment on day 6. This indicated that the two-step coagulation approach was able to effectively inhibit the growth of HepG2 xenografts and may result in tumor regression. In addition, the results revealed that mAb-SA alone could markedly affect tumor growth rate (mAb-SA vs. saline, $P < 0.05$). These results are supported by the final tumor weights (Fig. 8B) of mice in different treatment groups after treatment for 12 days.

***In vivo* intravascular thrombosis is observed following mAb-Sa:tTF-B treatment.** H&E staining was performed to

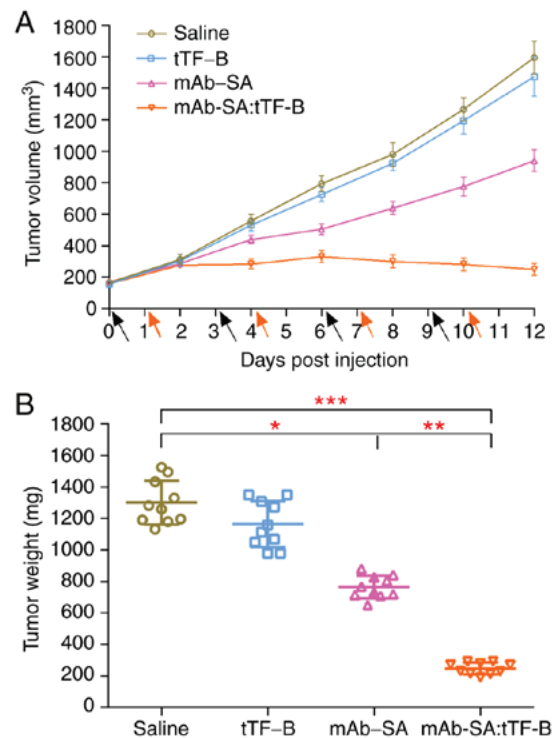


Figure 8. Antitumor efficiency studies on HepG2 tumor-bearing nude mouse models. (A) Mean tumor size was recorded for 12 days following the first treatment dose. Mice in various treatment groups received four intravenous injections of saline, mAb-SA, tTF-B, and mAb-SA:tTF-B at the indicated time (black arrows). Orange arrows indicate the time points at which the mAb-SA:tTF-B treatment group received tTF-B. (B) Mean tumor weight was evaluated after 12 days of treatment. * $P < 0.05$; ** $P < 0.01$; *** $P < 0.001$. mAb, monoclonal antibody; SA, streptavidin; tTF, truncated tissue factor; B, biotin.

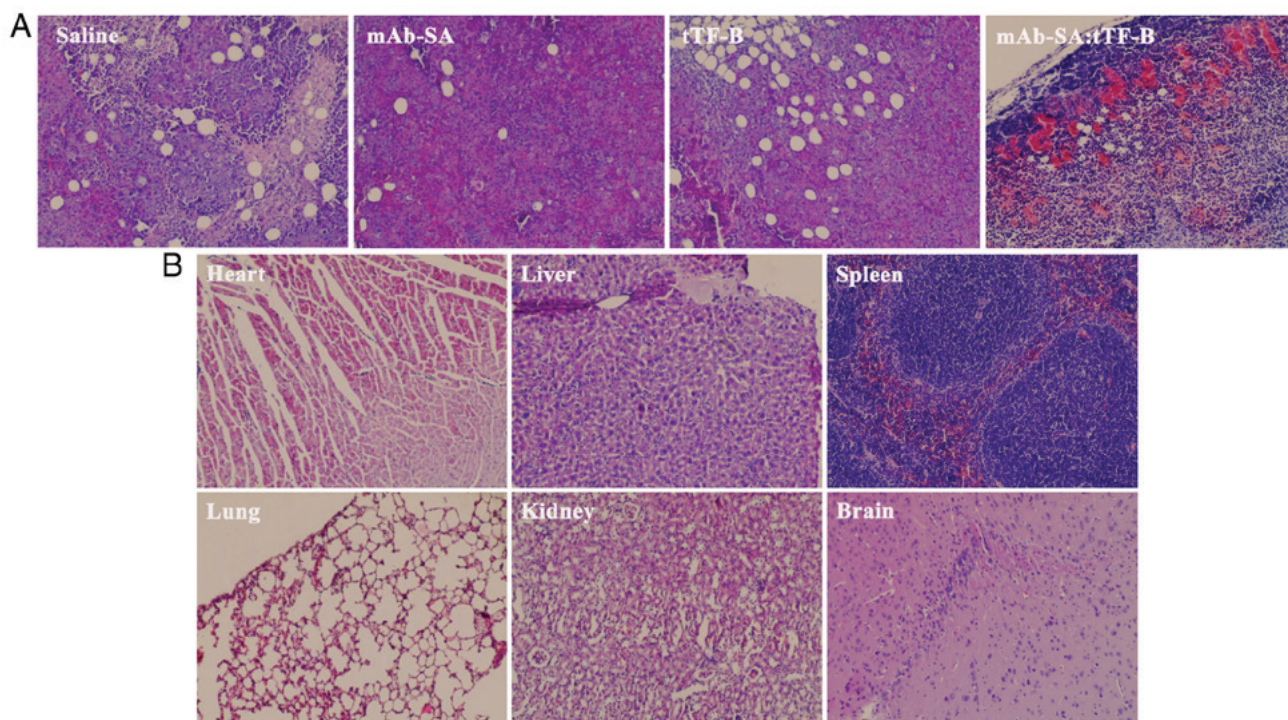


Figure 9. H&E staining of tumor tissues in nude mice and thrombotic risk evaluation in normal tissues of mAb-SA:tTF-B-treated mice. (A) H&E-stained tumor tissues from different treatment groups (magnification, x200). (B) H&E-stained normal tissues from the mAb-SA:tTF-B treatment group (magnification, x200). H&E, hematoxylin and eosin; mAb, monoclonal antibody; SA, streptavidin; tTF, truncated tissue factor; B, biotin.

observe histological changes in the tumor tissues of mice from the different treatment groups. Extensive thrombosis (estimated at ~80%) in blood vessels and necrosis were observed in the tumor tissues of mice treated with mAb-SA:tTF-B (Fig. 9A). In contrast, decreased intravascular embolization was exhibited in the other treatment groups. These results confirmed that the mAb-SA conjugate retained tumor vasculature-targeting ability and induced intravascular thrombosis *in vivo* by directing tTF-B to the vascular endothelial cell surface, thereby causing inhibition of tumor growth and promoting tumor regression. Major organs from the mAb-SA:tTF-B treatment group did not exhibit any visible ectopic embolism or overt tissue injury (Fig. 9B).

Discussion

Vascular targeting therapy was developed to selectively induce thrombosis in the vasculature of solid tumors. There are several advantages of this antitumor strategy (39). A local occlusion in the tumor vasculature may cause subsequent cell death due to the deprivation of adequate oxygen and nutrient supply. Drugs can also directly target universal tumor vascular endothelium cells in the blood; it has been reported that tumor vascular endothelial cells are unlikely to transform or acquire mutations (40). Therefore, this targeting therapy may be widely applicable. Conversely, conventional therapies, including chemotherapy and radiotherapy, although widely used, may exert cytotoxic effects on normal tissues (41,42). Numerous reports have demonstrated that the tTF ligand, which targets a specific antigen, can markedly inhibit tumor growth and promote tumor regression by selectively inducing intratumoral thrombosis (43-45); tTF has been conjugated with various

peptides to improve its efficacy, including SP5.2, NGR peptide and arginylglycylaspartic acid, or their derivatives. However, these fusion proteins require multiple administrations to achieve complete thrombosis in the tumor vasculature, which prevents the use of this strategy in clinical trials. This may be attributed to the target's low affinity for the targeting moiety and poor distribution (46). Therefore, to improve the antitumor efficacy of this ligand-directed approach, it is important to find a suitable tTF ligand delivery moiety and ensure it has a suitable tumor-specific receptor, which is also expressed in solid tumors.

NRP-1 is highly expressed in the endothelial cells of a variety of tumors, and exerts a positive effect on tumor angiogenesis, progression and metastasis (47-48). Therefore, the anti-NRP-1 mAb has been previously demonstrated to be a promising delivery method that may be used to target tumor vessels (14). To increase the concentration of tTF in tumor blood vessels and minimize its distribution in normal tissues, the present study introduced the SA/B system, which is characterized by high binding affinity.

In this approach, the preparation of mAb-SA conjugate was performed using EDC and sulfo-NHS. Sephadex G200 column chromatography was used to purify and unify the products. Native SDS-PAGE analysis was subsequently conducted to characterize the mAb-SA conjugate that was synthesized. The results indicated that a homogeneous conjugate product was obtained, with a theoretical molecular weight of ~210 kDa. A B-labeling kit was used to prepare tTF-B after the fusion protein tTF had been generated and purified. The *in vitro* activity of the mAb-SA:tTF-B system was tested prior to *in vivo* investigations. *In vitro* experiments, including confocal immunofluorescence, flow cytometry and factor X

activation, indicated that mAb-SA preserved the antibody's binding ability in HUVECs, which highly express NRP-1 (35). The results also demonstrated that tTF-B retained the ability to induce blood coagulation. Furthermore, the mAb-SA:tTF-B system was assessed using competitive ELISA, which demonstrated stable binding between mAb-SA and tTF-B. A subcutaneous tumor-bearing nude mouse model was established to identify the *in vivo* feasibility of the mAb-SA:tTF-B system. The *in vivo* distribution and tumor-targeting efficacy of mAb-SA was evaluated using live imaging. An intense fluorescent signal was observed in the tumor area after 3 h; this fluorescence persisted for 72 h. Conversely, weak fluorescence was observed in healthy organs. This suggested that mAb-SA was able to selectively target tumor tissues by interacting with NRP-1 on the vascular endothelial cell surface. In the antitumor activity studies, the mAb-SA conjugate was used to localize tumors, with the conjugate accumulating for 24 h until the concentration reached its peak. tTF-B was subsequently administered and captured by SA. Data from the growth inhibition assay demonstrated that tumor size decreased after day 6, and that the mean tumor volume and weight on day 12 were reduced compared with the other treatment groups. Histological analysis revealed that the mAb-SA:tTF-B system induced extensive thrombosis in tumor vessels. No visible ectopic embolism or injury was observed in normal organs, which reflects the robust biological targeting ability of this system.

In conclusion, an antitumor composite system based on vascular targeting was successfully constructed in the present study. *In vitro* experiments and *in vivo* studies demonstrated that the mAb-SA:tTF-B system effectively inhibited tumor growth and promoted tumor regression by selectively targeting tumor blood vessels and inducing complete vascular infarction. The introduction of the SA/B system is a promising approach for improving tTF-ligand coagulation efficiency and antitumor activity. Therefore, the present study may provide novel insight for the development of vasculature-targeting antitumor treatments.

Acknowledgements

Not applicable.

Funding

This study was supported by the National Natural Science Foundation of China (grant. nos. 81773770) and the Science and Technology Foundation of Fujian Province, China (grant nos. 2018R1036-1, 2018R1036-3 and 2019R1001-2).

Availability of data and materials

The datasets generated and analyzed during the present study are available from the corresponding author upon reasonable request.

Authors' contributions

PX drafted the manuscript. PX, MZ and SW performed the experiments. JY, FL, TW and PX designed the study. TL, CL,

LiW and LaW performed data analysis. JY and PX contributed to the manuscript revisions. All authors reviewed the manuscript. All authors have read and approved the final version of the manuscript for publication.

Ethics approval and consent to participate

All the animal experiments performed in this study were approved by the Ethics Committee of Xiamen University.

Patient consent for publication

Not applicable.

Competing interests

The authors declare that they have no competing interests.

References

- Folkman J: The role of angiogenesis in tumor growth. *Semin Cancer Biol* 3: 65-71, 1992.
- Blumberg N: Tumor angiogenesis factor. Speculations on an approach to cancer chemotherapy. *Yale J Biol Med* 47: 71-81, 1974.
- Milowsky MI, Nanus DM, Kostakoglu L, Sheehan CE, Vallabhajosula S, Goldsmith SJ, Ross JS and Bander NH: Vascular targeted therapy with anti-prostate-specific membrane antigen monoclonal antibody J591 in advanced solid tumors. *J Clin Oncol* 25: 540-547, 2007.
- Bose D, Meric-Bernstam F, Hofstetter W, Reardon DA, Flaherty KT and Ellis LM: Vascular endothelial growth factor targeted therapy in the perioperative setting: Implications for patient care. *Lancet Oncol* 11: 373-382, 2010.
- Kessler T, Bieker R, Padró T, Schwöppe C, Persigehl T, Bremer C, Kreuter M, Berdel WE and Mesters RM: Inhibition of tumor growth by RGD peptide-directed delivery of truncated tissue factor to the tumor vasculature. *Clin Cancer Res* 11: 6317-6324, 2005.
- Schwöppe C, Kessler T, Persigehl T, Liersch R, Hintelmann H, Dreischalück J, Ring J, Bremer C, Heindel W, Mesters RM and Berdel WE: Tissue-factor fusion proteins induce occlusion of tumor vessels. *Thromb Res* 125 (Suppl 2): S143-S150, 2010.
- Furie B and Furie BC: The molecular basis of coagulation. *Cell* 53: 505-518, 1988.
- Persigehl T, Ring J, Bremer C, Heindel W, Holtmeier R, Stypmann J, Claesener M, Hermann S, Schäfers M, Zerbst C, *et al*: Non-invasive monitoring of tumor-vessel infarction by retargeted truncated tissue factor tTF-NGR using multi-modal imaging. *Angiogenesis* 17: 235-246, 2014.
- Alessi P, Ebbinghaus C and Neri D: Molecular targeting of angiogenesis. *Biochim Biophys Acta* 1654: 39-49, 2004.
- Archer R, Wakabayashi M, Sevilla R, Summers S, King S and Aimes R: Targeting truncated tissue factor with tumor vasculature specific monoclonal antibodies: Developing coaguligands as cancer therapeutics. *Cancer Res* 67: 14-18, 2007.
- Kessler T, Schwöppe C, Liersch R, Schliemann C, Hintelmann H, Bieker R, Berdel WE and Mesters RM: Generation of fusion proteins for selective occlusion of tumor vessels. *Curr Drug Discov Technol* 5: 1-8, 2008.
- Soker S, Takashima S, Miao HQ, Neufeld G and Klagsbrun M: Neuropilin-1 is expressed by endothelial and tumor cells as an isoform-specific receptor for vascular endothelial growth factor. *Cell* 92: 735-745, 1998.
- Wise LM, Veikkola T, Mercer AA, Savory LJ, Fleming SB, Caesar C, Vitali A, Makinen T, Alitalo K and Stacker SA: Vascular endothelial growth factor (VEGF)-like protein from orf virus NZ2 binds to VEGFR2 and neuropilin-1. *Proc Natl Acad Sci USA* 96: 3071-3076, 1999.
- Gagnon ML, Bielenberg DR, Gechtman Z, Miao HQ, Takashima S, Soker S and Klagsbrun M: Identification of a natural soluble neuropilin-1 that binds vascular endothelial growth factor: In vivo expression and antitumor activity. *Proc Natl Acad Sci USA* 97: 2573-2578, 2000.

15. Bergé M, Allanic D, Bonnin P, de Montrion C, Richard J, Suc M, Boivin JF, Contrères JO, Lockhart BP, Pocard M, *et al.*: Neuropilin-1 is upregulated in hepatocellular carcinoma and contributes to tumour growth and vascular remodelling. *J Hepatol* 55: 866-875, 2011.
16. Seifi-Alan M, Shams R, Bandehpour M, Mirfakhraie R and Ghafouri-Fard S: Neuropilin-1 expression is associated with lymph node metastasis in breast cancer tissues. *Cancer Manag Res* 10: 1969-1974, 2018.
17. Huang X, Molema G, King S, Watkins L, Edgington TS and Thorpe PE: Tumor infarction in mice by antibody-directed targeting of tissue factor to tumor vasculature. *Science* 275: 547-550, 1997.
18. Thorpe PE: Vascular targeting agents as cancer therapeutics. *Clin Cancer Res* 10: 415-427, 2004.
19. Hu P, Yan J, Sharifi J, Bai T, Khawli LA and Epstein AL: Comparison of three different targeted tissue factor fusion proteins for inducing tumor vessel thrombosis. *Cancer Res* 3: 5046-5053, 2003.
20. Saga T, Weinstein JN, Jeong JM, Heya T, Lee JT, Le N, Paik CH, Sung C and Neumann RD: Two-Step targeting of experimental lung metastases with biotinylated antibody and radiolabeled streptavidin. *Cancer Res* 54: 2160-2165, 1994.
21. Zhang M, Sakahara H, Yao Z, Saga T, Nakamoto Y, Sato N, Nakada H, Yamashina I and Konishi J: Intravenous avidin chase improved localization of radiolabeled streptavidin in intraperitoneal xenograft pretargeted with biotinylated antibody. *Nucl Med Biol* 24: 61-64, 1997.
22. Sakahara H and Saga T: Avidin-biotin system for delivery of diagnostic agents. *Adv Drug Deliv Rev* 37: 89-101, 1999.
23. Liu X, Yang Q, Nakamura C and Miyake J: Avidin-biotin-immobilized liposome column for chromatographic fluorescence on-line analysis of solute-membrane interactions. *J Chromatogr B Biomed Sci Appl* 750: 51-60, 2001.
24. Medina LA, Calixto SM, Klipper R, Phillips WT and Goins B: Avidin/biotin-liposome system injected in the pleural space for drug delivery to mediastinal lymph nodes. *J Pharm Sci* 93: 2595-2608, 2004.
25. Nobs L, Buchegger F, Gurny R and Allemann E: Biodegradable nanoparticles for direct or two-step tumor immunotargeting. *Bioconjug Chem* 17: 139-145, 2006.
26. Kheiruloomoom A, Dayton PA, Lum AF, Little E, Paoli EE, Zheng H and Ferrara KW: Acoustically-active microbubbles conjugated to liposomes: Characterization of a proposed drug delivery vehicle. *J Control Release* 118: 275-284, 2007.
27. Goldenberg DM, Sharkey RM, Paganelli G, Barbet J and Chatal JF: Antibody pretargeting advances cancer radioimmunodetection and radioimmunotherapy. *J Clin Oncol* 24: 823-834, 2006.
28. Urbano N, Papi S, Ginanneschi M, De Santis R, Pace S, Lindstedt R, Ferrari L, Choi S, Paganelli G and Chinol M: Evaluation of a new biotin-DOTA conjugate for pretargeted antibody-guided radioimmunotherapy (PAGRIT). *Eur J Nucl Med Mol Imaging* 34: 68-77, 2007.
29. Zeng F, Luo F, Lv S, Zhang H, Cao C, Chen X, Wang S, Li Z, Wang X, Dou X, *et al.*: A monoclonal antibody targeting neuropilin-1 inhibits adhesion of MCF7 breast cancer cells to fibronectin by suppressing the FAK/p130cas signaling pathway. *Anticancer Drugs* 25: 663-672, 2014.
30. Chen F, Nielsen S and Zenobi R: Understanding chemical reactivity for homo- and heterobifunctional protein cross-linking agents. *J Mass Spectrom* 48: 807-812, 2013.
31. Nwe K, Milenic DE, Ray GL, Kim YS and Brechbiel MW: Preparation of cystamine core dendrimer and antibody-dendrimer conjugates for MRI angiography. *Mol Pharm* 9: 374-381, 2012.
32. Neerman MF, Zhang W, Parrish AR and Simanek EE: In vitro and in vivo evaluation of a melamine dendrimer as a vehicle for drug delivery. *Int J Pharm* 281: 129-132, 2004.
33. Chan EC and Ho PC: Preparation and characterization of immunogens for antibody production against metanephrine and normetanephrine. *J Immunol Methods* 266: 143-154, 2002.
34. Xu ZC, Shen HX, Chen C, Ma L, Li WZ, Wang L and Geng ZM: Neuropilin-1 promotes primary liver cancer progression by potentiating the activity of hepatic stellate cells. *Oncol Lett* 15: 2245-2251, 2018.
35. Wang L, Zeng H, Wang P, Soker S and Mukhopadhyay D: Neuropilin-1-mediated vascular permeability Factor/Vascular endothelial growth Factor-dependent endothelial cell migration. *J Biol Chem* 278: 48848-48860, 2003.
36. Chen X, Lv H, Ye M, Wang S, Ni E, Zeng F, Cao C, Luo F and Yan J: Novel superparamagnetic iron oxide nanoparticles for tumor embolization application: Preparation, characterization and double targeting. *Int J Pharm* 426: 248-255, 2012.
37. Hylarides MD, Mallett RW and Meyer DL: A robust method for the preparation and purification of Antibody/streptavidin conjugates. *Bioconjug Chem* 12: 421-427, 2001.
38. Liao MY, Kuo MY, Lu TY, Wang YP and Wu HC: Generation of an anti-EpCAM antibody and epigenetic regulation of EpCAM in colorectal cancer. *Int J Oncol* 46: 1788-1800, 2015.
39. Gottstein C, Wels W, Ober B and Thorpe PE: Generation and characterization of recombinant vascular targeting agents from hybridoma cell lines. *Biotechniques* 30: 190-194, 2001.
40. Hu Z, Rao B, Chen S and Duanmu J: Selective and effective killing of angiogenic vascular endothelial cells and cancer cells by targeting tissue factor using a factor VII-targeted photodynamic therapy for breast cancer. *Breast Cancer Res Treat* 126: 589-600, 2011.
41. Rades D, Fehlauer F, Bajrovic A, Mahlmann B, Richter E and Alberti W: Serious adverse effects of amifostine during radiotherapy in head and neck cancer patients. *Radiother Oncol* 70: 261-264, 2004.
42. Monsuez JJ, Charniot JC, Vignat N and Artigou JY: Cardiac side-effects of cancer chemotherapy. *Int J Cardiol* 144: 3-15, 2010.
43. Dienst A, Grunow A, Unruh M, Rabausch B, Nör JE, Fries JW and Gottstein C: Specific occlusion of murine and human tumor vasculature by VCAM-1-targeted recombinant fusion proteins. *J Natl Cancer Inst* 97: 733-747, 2005.
44. Bieker R, Kessler T, Schwöppe C, Padró T, Persigehl T, Bremer C, Dreischalück J, Kolkmeier A, Heindel W, Mesters RM and Berdel WE: Infarction of tumor vessels by NGR-peptide-directed targeting of tissue factor: Experimental results and first-in-man experience. *Blood* 113: 5019-5027, 2009.
45. Lv S, Ye M, Wang X, Chen X, Dou X, Dai Y, Dai Y, Zeng F, Luo L, Wang C, *et al.*: A recombinant fusion protein SP5.2/tTF induce thrombosis in tumor blood vessel. *Neoplasma* 62: 531-540, 2015.
46. Schmidt LH, Stucke-Ring J, Brand C, Schliemann C, Harrach S, Muley T, Herpel E, Kessler T, Mohr M, Görlich D, *et al.*: CD13 as target for tissue factor induced tumor vascular infarction in small cell lung cancer. *Lung Cancer* 113: 121-127, 2017.
47. Pan Q, Chanthery Y, Liang WC, Stawicki S, Mak J, Rathore N, Tong RK, Kowalski J, Yee SF, Pacheco G, *et al.*: Blocking neuropilin-1 function has an additive effect with anti-VEGF to inhibit tumor growth. *Cancer Cell* 11: 53-67, 2007.
48. Grandclement C and Borg C: Neuropilins: A new target for cancer therapy. *Cancers (Basel)* 3: 1899-1928, 2011.



This work is licensed under a Creative Commons Attribution-NonCommercial-NoDerivatives 4.0 International (CC BY-NC-ND 4.0) License.